Electronic Supplementary Material (ESI) for Green Chemistry.

This journal is © The Royal Society of Chemistry 2022

Supplementary Information

Efficient Heterogeneous Photocatalytic C-C Coupling of Halogenated Arenes Mediated by Metal Cocatalyst

Yaru Li,[a,b,c] Yajiao Li,[a] Caixia Hu,[d] Xiaodong Wen,[b,c,d] Hongwei Xiang,[b,d] Yongwang Li,[b,d] Hans Niemantsverdriet,[d,e] and Ren Su*[a,d]

[a] Soochow Institute for Energy and Materials InnovationS (SIEMIS), Key Laboratory of Advanced Carbon Materials and Wearable Energy, Technologies of Jiangsu Province, Soochow University, Suzhou, 215006, China.

[b] State Key Laboratory of Coal Conversion, Institute of Coal Chemistry, CAS, Taiyuan, 030001, China.

[c] University of Chinese Academy of Sciences, Beijing, 100049, China.

[d] SynCat@Beijing, Synfuels China Technology Co. Ltd., Leyuan South Street II, No.1, Yanqi Economic Development Zone C#, Huairou District, Beijing, 101407, China.

[e] SynCat@DIFFER, Syngaschem BV, 6336 HH Eindhoven, The Netherlands.

AUTHOR INFORMATION

Corresponding Authors

* suren@suda.edu.cn (R. Su)

Table of Contents

Experimental Procedures

Supporting Figures

Figure S1. Diagram of the reactor for photo-deposition of metal nanoparticles on gCN.

Figure S2. Characterizations of the pristine gCN, Ni/gCN, Cu/gCN and Pd/gCN photocatalysts.

Figure S3. GC-MS analysis of radical species.

Figure S4. GC and MS analysis of photocatalytic benzyl bromide conversion using different photocatalysts.

Figure S5-S36. Product analysis of photocatalytic conversion of benzyl bromide derivatives using Ni/gCN photocatalyst by GC, MS and NMR.

Supporting Tables

Table S1. ICP-AES analysis of metal loadings on gCN.

Table S2. Blank tests for photocatalytic homocoupling of benzyl bromide.

Table S3. Survey of solvent for photocatalytic benzyl bromide conversion.

Supporting References

Experimental Procedures

Supporting Figures

1. Synthesis of metal/gCN photocatalysts.

The graphitic carbon nitride (gCN) was synthesized using urea as the precursor. 40 g of urea was loaded into a 100 mL crucible with a lid and calcined in a muffle oven from 50 ^{o}C to 550 ^{o}C for 3 h with a ramping rate of 5 $^{o}C \cdot min^{-1}$. Then it was cooled to room temperature (RT) to obtain the yellow gCN sample.

The Ni, Cu, Au, Ag, Pt, Pd, Rh and Ru nanoparticles (NPs) were supported on gCN *via* a modified photo-deposition method. We describe the deposition of 1.0 wt% Pd on gCN as an example. Firstly, 500 mg of gCN powders were dispersed into an isopropanol-water solution (15 mL of isopropanol and 10 mL of water) and was sonicated for 10 min to form a homogeneous suspension. Then 9 mg of $PdCl_2$ powder was added to the prepared gCN suspension under continuous stirring. The suspension was evacuated and purged by N_2 gas 3 times to remove dissolved O_2 using a home-build vacuum line system (Figure. S1). The suspension was eventually irradiated using a 365 nm LED light source (Spectroline TRITAN 365) for 2 h at RT under vacuum conditions to reduce Pd cations into metallic Pd. Finally, the suspension was filtered and washed by deionized water three times, and dried at 80 ^{o}C for 3 h in a vacuum oven.

The deposition of 1.0 wt% Fe on gCN was carried out by an impregnation method. Firstly, 500 mg of gCN powder was dispersed into 20 mL of water and sonicated for 20 min to form a homogeneous suspension. Then 36.6 mg of $Fe(NO_3)_3 \cdot 9H_2O$ powder was added into the gCN

suspension under continuous stirring for 2 h. The suspension was filtered, dried and calcined in a muffle oven at 350 ^{o}C for 3 h with a ramping rate of 5 ^{o}C·min^{-1} under air atmosphere. Finally, the Fe/gCN was obtained. The deposition of Co is also realized using this method using a calcination temperature of 300 ^{o}C.

$HAuCl_4 \cdot 4H_2O$, $AgNO_3$, $CuCl_2 \cdot 2H_2O$, H_2PtCl_6, $PdCl_2$, $Ni(NO_3)_2 \cdot 6H_2O$, $Fe(NO_3)_3 \cdot 9H_2O$, $RuCl_3 \cdot xH_2O$, $RhCl_3 \cdot 3H_2O$ and $Co(NO_3)_2 \cdot 6H_2O$ were employed as the metal source to deposit the respective metals on gCN. The loading of the metals was determined by inductively coupled plasma-atomic emission spectroscopy (ICP-AES) analysis (Table S1).

2. Powder X-ray Diffraction (PXRD). The XRD patterns were recorded on a Bruker D8 Advance diffractometer with a step size of 0.04°, a scan rate of 0.1°·s^{-1}, and a scan range of 5° to 60° using a Cu-Kα radiation source (40 kV, 40 mA). Figure. S2 shows the PXRD patterns of all fresh samples. All diffraction peaks of the sample can be indexed to gCN. The diffraction peaks of metal cannot be detected due to the detection limit of XRD. The loading of metal does not influence the crystalline structure of gCN.[1]

3. High Resolution Transmission Electron Microscope (HRTEM). The morphology of samples was obtained by using a Talos TALOS F200A. The powder samples were dispersed into ethanol and dropped on the Cu grid for analysis.

4. X-ray Photoelectron Spectroscopy (XPS). The chemical composition and oxidation state of the elements on the catalyst surface were characterized by an X-ray photoelectron spectrometer

equipped with an Al Kα X-ray source (K-alpha, Thermo Fisher Scientific, USA). Survey scans were measured from 1100 to -10 eV using a pass energy of 160 eV with a step size of 1 eV and a dwell time of 0.1 s, whereas the spectra of C1s, N1s and Ni2p were collected in the desired energy regions using a pass energy of 40 eV with a step size of 0.1 eV and a dwell time of 0.5 s. The C1s binding energy of adventitious carbon (284.6 eV) was used for calibration.

5. Diffuse reflectance spectroscopy (DRS). The DRS were recorded using a photospectrometer (UH4150, Hitachi) equipped with a spherical integrating detector to analyze the optical properties of the photocatalysts. The spectra were obtained from 200 to 800 nm using spectroscopy grade $BaSO_4$ as the reference.

6. Fourier transform infrared (FTIR) spectrometer. FTIR spectra were used to analyze the absorption bands of the photocatalysts (VERTEX 70, Bruker).

7. Photoluminescence Spectroscopy (PL). Photoluminescence spectra were measured on an Edinburgh fluorescence photometer (FLS 1000) using a xenon lamp with a wavelength of 375 nm.

8. Temperature-programmed desorption (TPD). We analyzed the adsorption and dissociation of benzyl bromide on different catalysts by TPD using a chemisorption analyzer (AutoChem II) coupled with an MS (OmniStar GSD, Pfeiffer). The procedure of TPD analysis is described below: Prepare 40 mg fresh photocatalyst powders in a closed chamber. Then, benzyl bromide was bubbled into the chamber using Ar as the carrier gas, flowing for 1h during which the chamber was sealed to make sure the surface of the photocatalyst is saturated with benzyl bromide. Finally,

the signal of m/z = 91 was collected as the sample was heated from 30 °C to 500 °C with a ramping rate of 10 °C·min^{-1}, using He as the carrier gas.

9. Identification of $Br^{\bullet}$ and Br_2. UV-vis absorption spectra (UH4150, Hitachi) were used to confirm the formation of $Br^{\bullet}$ and molecular bromine. 1,3,5-trimethoxybenzene (TMB) is used to titrate the formation of $Br^{\bullet}$ according to the following equation from the literature:[2]

$$Br^{\bullet} + TMB \rightarrow TMB^{\bullet+} + Br^{-} \qquad \text{Eq. S1}$$

An absorption peak at ~570 nm is associated to the formation of the $TMB^{\bullet+}$ radicals.

In practical, 15 mg of photocatalyst was added in a 1.5 mL of isopropanol solution that contains 160 mM of benzyl bromide and 320 mM of TMB to perform the analysis. A 420 nm LED was used as the light source. The reaction suspension was centrifuged and analyzed by UV-vis spectrometer.

The absorption peak at ~470 nm is used to characterize the evolution of Br_2 upon irradiation. In practical, 15 mg of photocatalyst was added in a 1.5 mL of isopropanol solution that contains 160 mM of benzyl bromide to perform the analysis.

10. Identification of Br^-. The ionic conductivity of the reaction solution is determined using a HQ440d multi analyzer (Hach) to probe the evolution of Br anions.

11. Hydrogen production during reaction. The evolution of gas-phase products was determined by a quadruple mass spectrometer (QMS, HPR-20, Hiden) equipped with an *in-situ* reactor. Details of experimental procedures and quantitative analysis methods can be found in our previous

publications.[3] The mass to charge ratio (m/e^-) of 2 are measured to monitor the evolution of hydrogen.

The hydrogen evolution was calculated according to Equations. S(2) and S(3):

$$p(H_2)_{reactor} = RSF(H_2) \times p(H_2)_{detector} \times p(Air)_{reactor} / p(Air)_{detector} \quad \text{Eq. S2}$$

$$n(H_2) = p(H_2)_{reactor} \times V_{reactor} / RT \quad \text{Eq. S3}$$

where

$p(H_2)_{reactor}$ is the partial pressure of H_2 in the reaction chamber;

$RSF(H_2)$ is the relative sensitivity factor of H_2 (0.4 in ambient);

$p(H_2)_{detector}$ is the partial pressure of H_2 detected by the mass spectrometer;

$p(Air)_{reactor}$ is the pressure of air in the reaction chamber (100 kPa);

$p(Air)_{detector}$ is the pressure of air ($N_2 + O_2$) detected by the mass spectrometer;

$n(H_2)$ is the amount of H_2 evolution in the reaction chamber;

$V_{reactor}$ is the volume of the chamber excluding the liquid volume (286 mL);

$R = 8.314\ J \cdot mol^{-1} \cdot K^{-1}$, $T = 298\ K$.

12. Continuous flow synthesis of bibenzyl using the Ni/gCN. 60 mg of Ni/gCN and 50 mg of silica gel (63-200 μm particle size) were mixed and grounded in a mortar, and then mixed with 950 mg of a 1:1 mixture of silica gel (63-200 μm particle size) and glass beads (250-500 μm). The catalyst powders were then filled in a 70 cm long fluorinated ethylene propylene (FEP) tubing (internal diameter: 3 mm, wall thickness: 0.5 mm), which was equipped with a cotton filter in the outlet. The tubing was fixed on the supporter (measuring cylinder) and wrapped by an aluminum foil to reflect the scattered light. A 80 mL of the substrate containing solution (8 mM benzyl

bromide in isopropanol) was injected into the reactor using a syringe pump (flow rate: 0.11 $mL \cdot min^{-1}$). The liquid phase products were collected and analyzed by gas chromatography (GC).

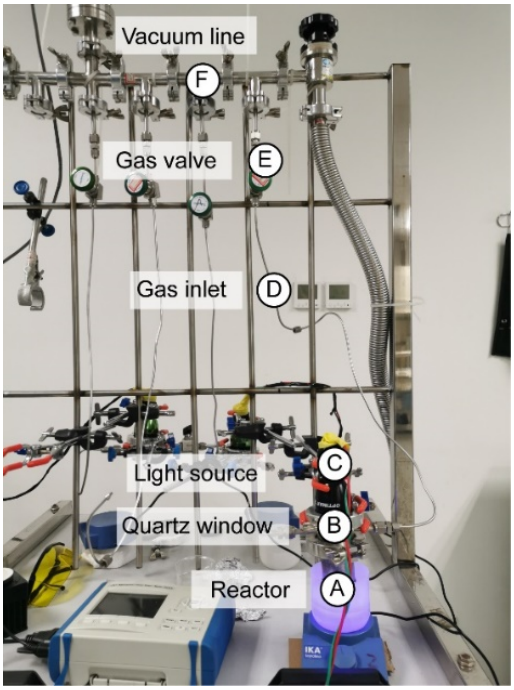

Figure S1. Diagram of the reactor for photodeposition of metal nanoparticles on gCN.

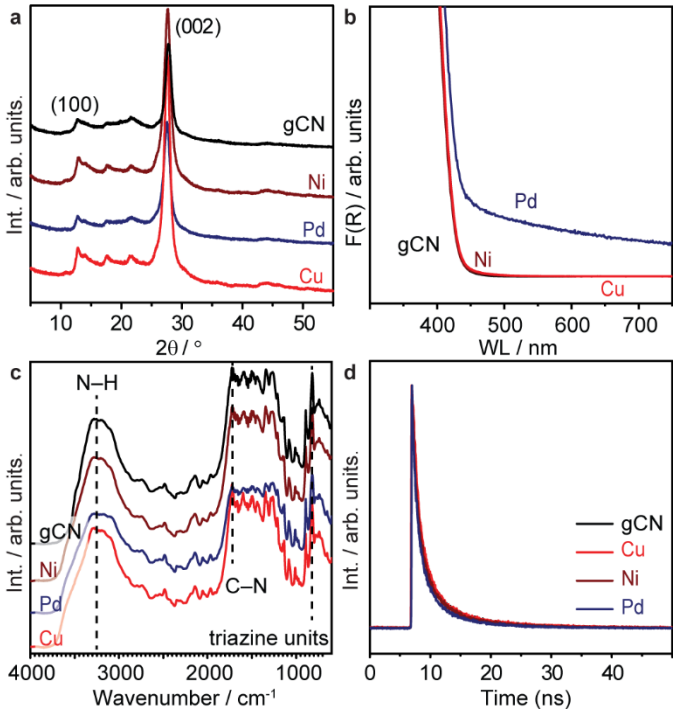

Figure S2. Characterizations of the pristine gCN, Ni/gCN Cu/gCN, and Pd/gCN photocatalysts. **a.** PXRD patterns. **b.** DRS spectra. **c.** FTIR spectra. **d.** Time resolved photoluminescence spectra.

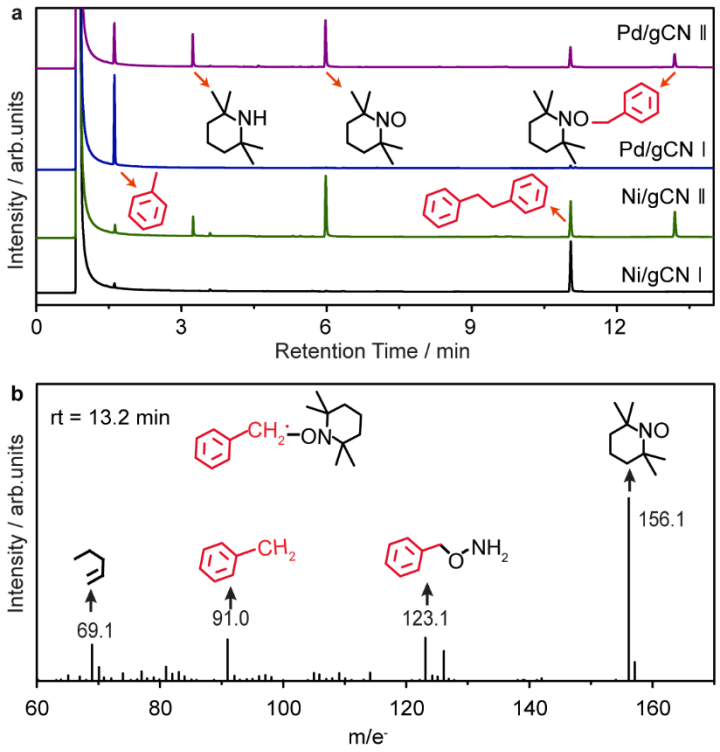

Figure S3. (a) and (b) GC-MS analysis of radical species evolved during photocatalytic benzyl bromide conversion using TEMPO as a radical trap (16 mM). The Ni/gCN I and Pd/gCN I represents the reaction without TEMPO, the Ni/gCN II and Pd/gCN II represents the reaction with TEMPO, respectively. (b) MS spectra of the Ni/gCN II.

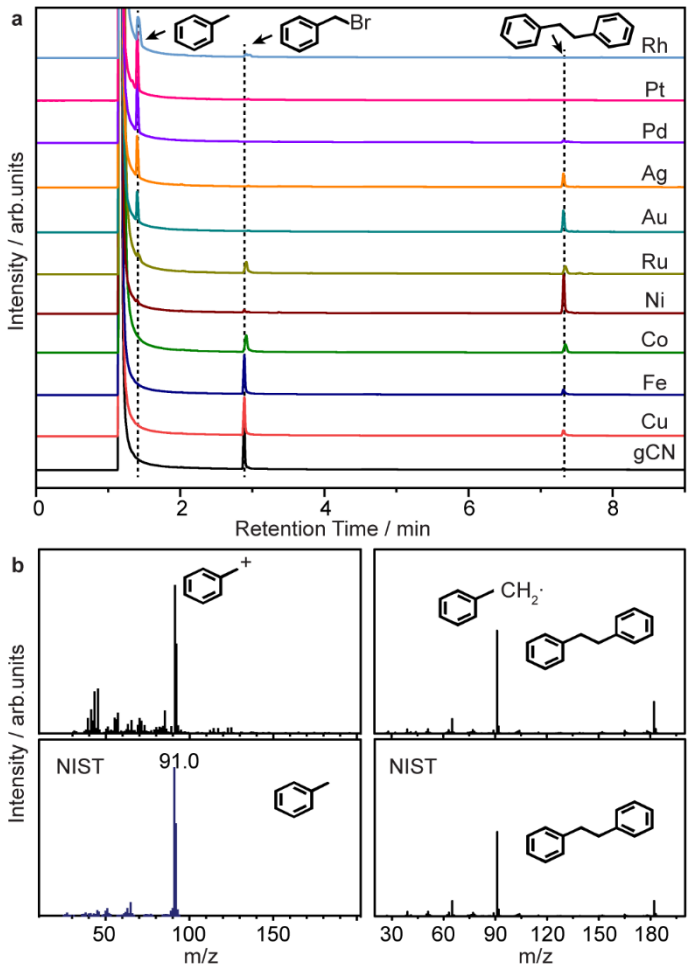

Figure S4. GC and MS analysis of photocatalytic benzyl bromide conversion using different photocatalysts.

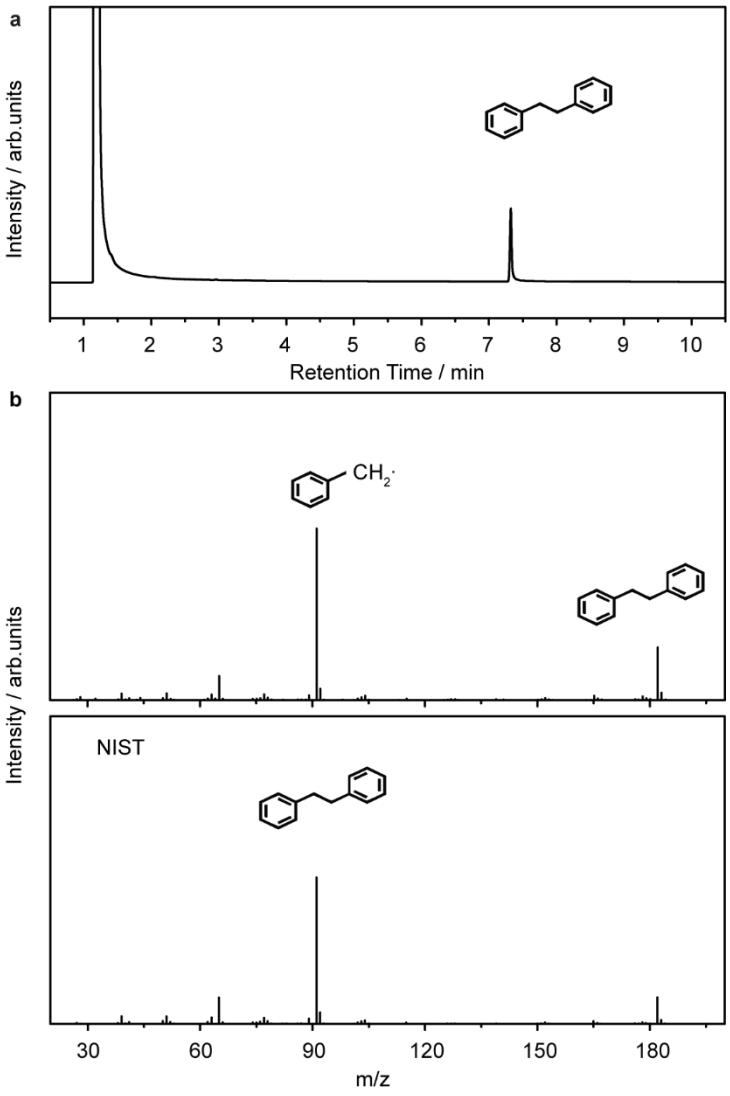

Figure S5. Benzyl bromide as substrate. **a** GC data. **b** MS data.

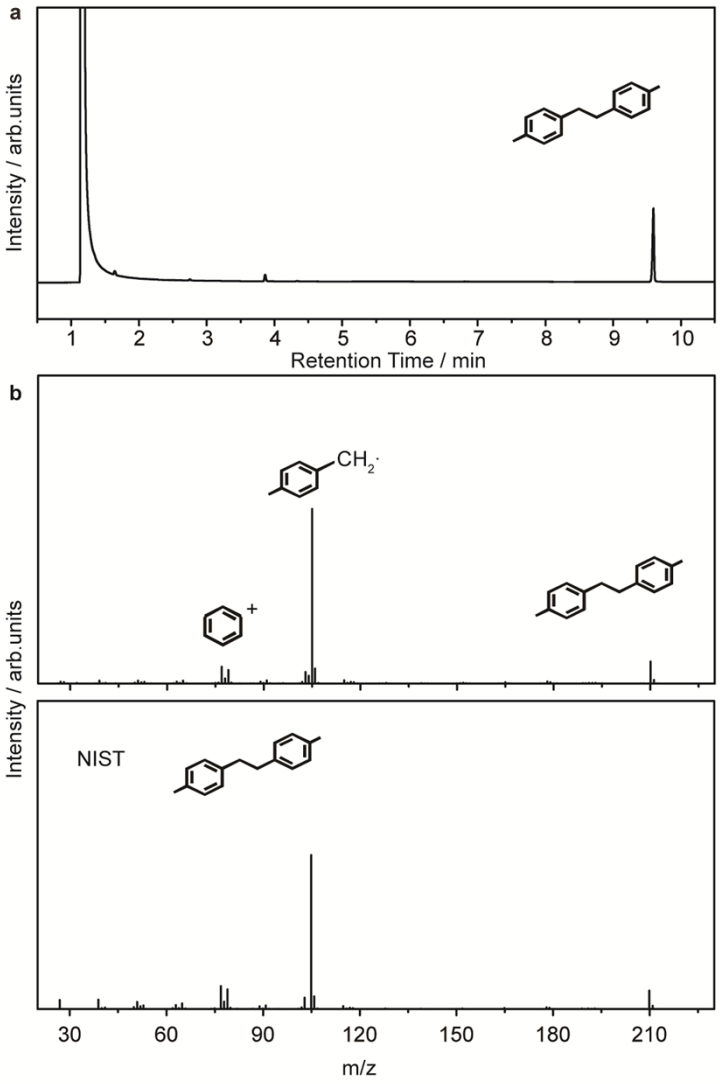

Figure S6. 4-methylbenzyl bromide as substrate. **a** GC data. **b** MS data.

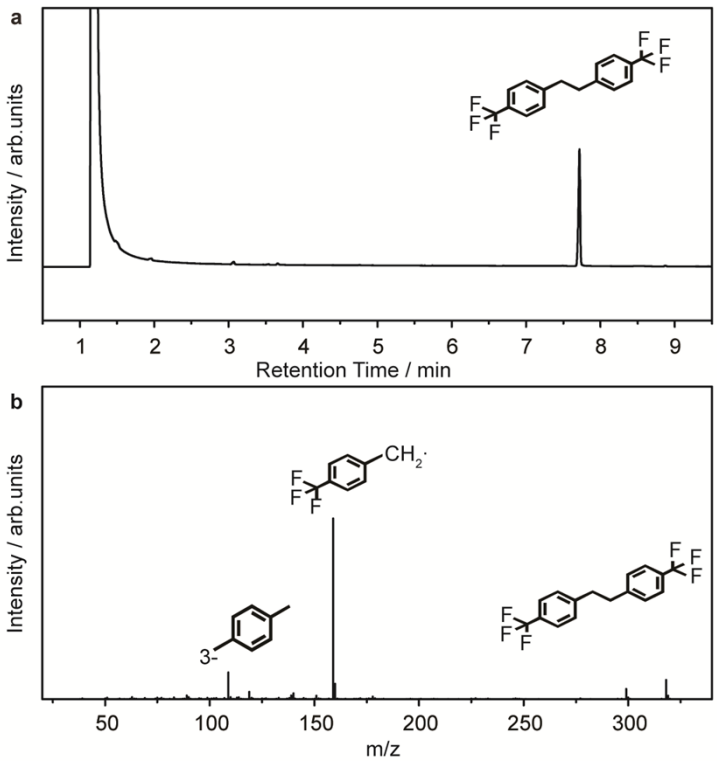

Figure S7. 4-trifluoromethylbenzyl bromide as substrate. **a** GC data. **b** MS data.

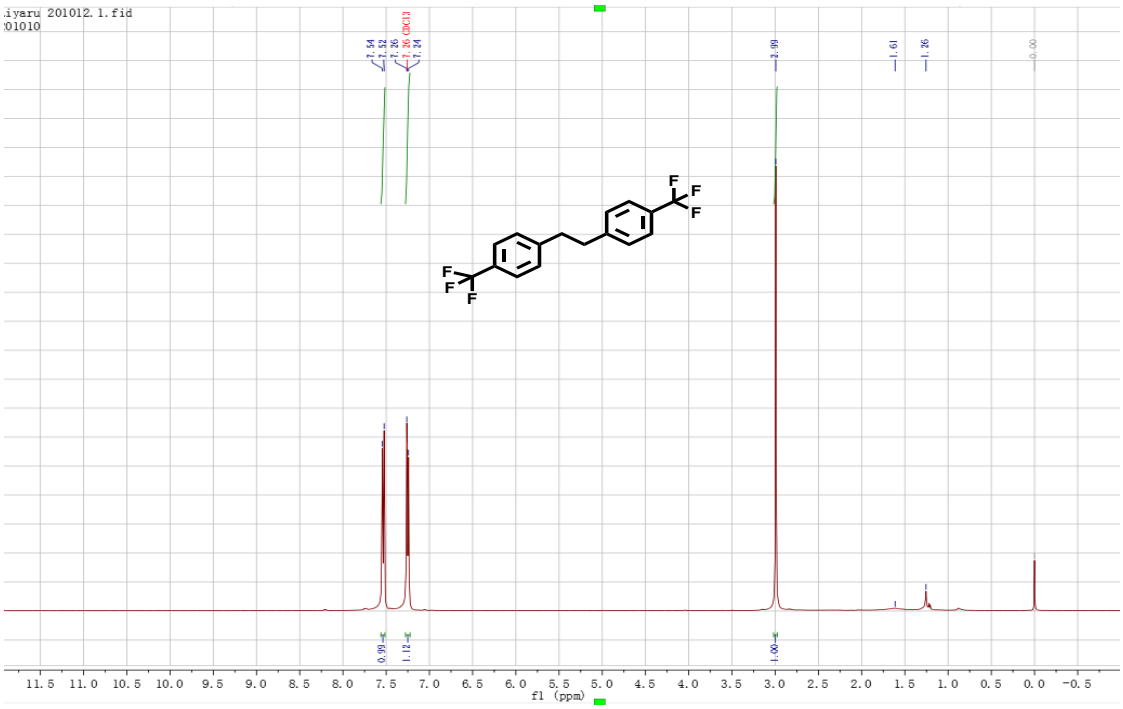

Figure S8. H spectrum (4-trifluoromethylbenzyl bromide as substrate). Reaction conditions: 8 mM of reactant, 100 mg catalyst, 15 mL isopropanol solution under vacuum, 420 nm LED lamp irradiated for 2 h, 29.5 $mW \cdot cm^{-2}$. Organic solutions were concentrated under reduced pressure on an evaporator using water bath for volatile compounds. ^1H NMR (400 MHz, $CDCl_3$) δ 7.54-7.52 (s, 1H), 7.26-7.24 (s, 1H), 2.99 (s, 1H). (Note: $CDCl_3$ referenced at 7.26 and 77.04 ppm respectively). Data for ^1H NMR are reported as follows: chemical shift (δ ppm), multiplicity (s = singlet, d = doublet, t = triplet, q = quartet, m = multiplet), integration, and coupling constant (Hz)).

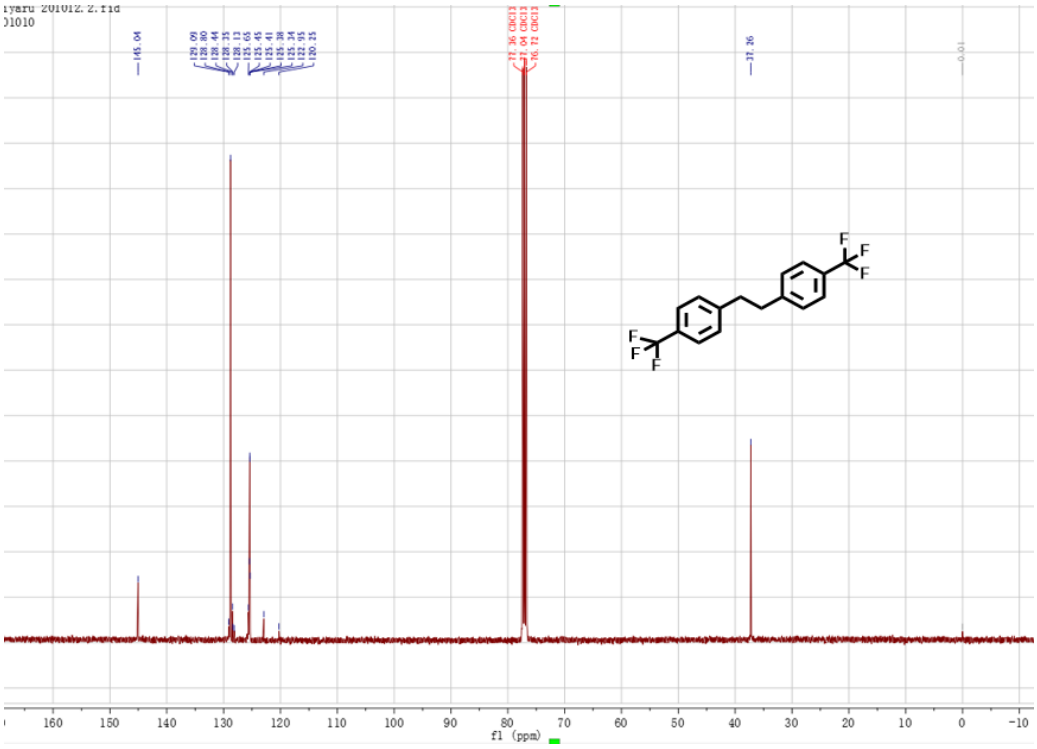

Figure S9. C spectrum (4-trifluoromethylbenzyl bromide as substrate). ^{13}C NMR (100 MHz, $CDCl_3$) δ145.04, 128.80, 125.41, 122.95, 37.26.

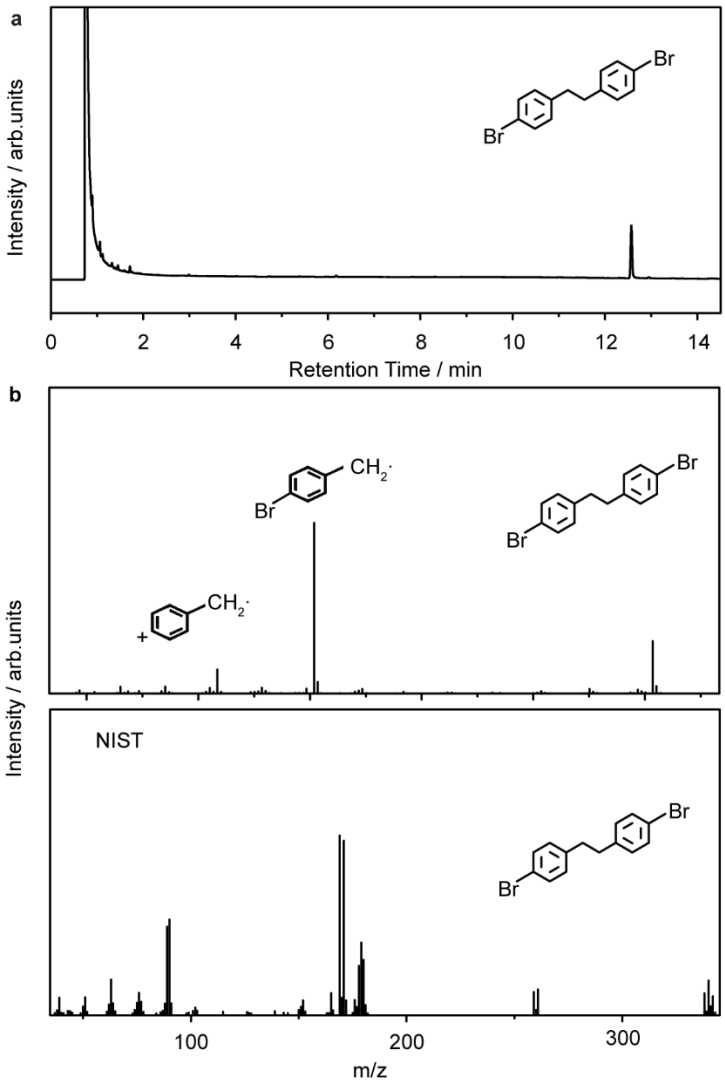

Figure S10. 4-bromobenzyl bromide as substrate. **a** GC data. **b** MS data.

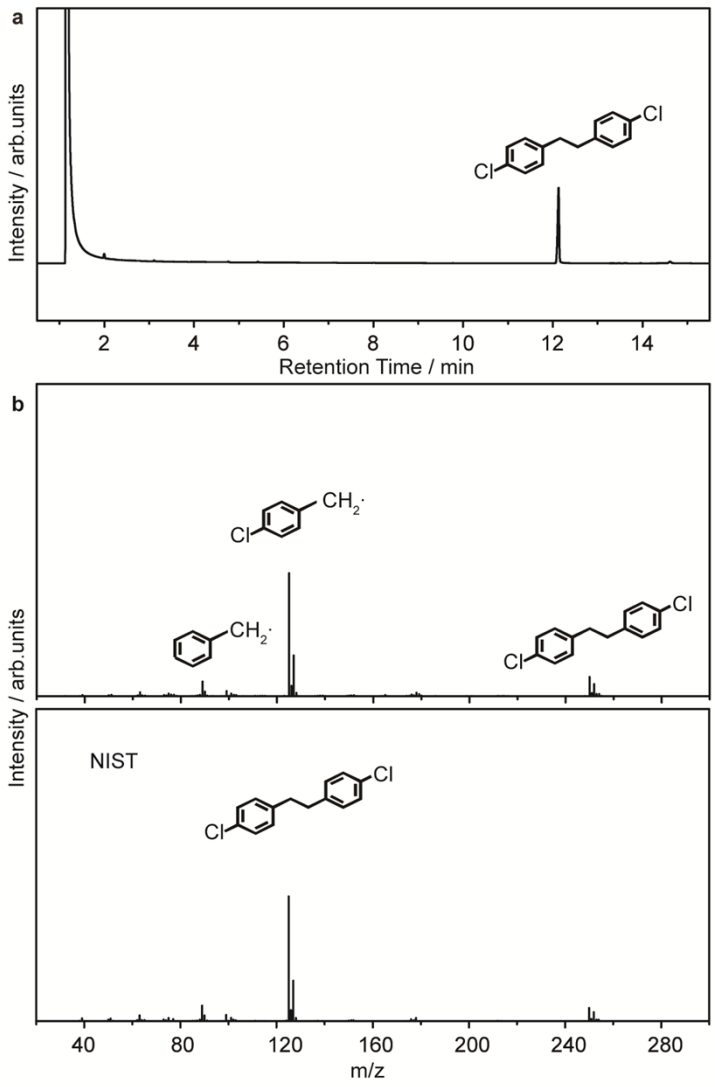

Figure S11. 4-chlorobenzyl bromide as substrate. **a** GC data. **b** MS data.

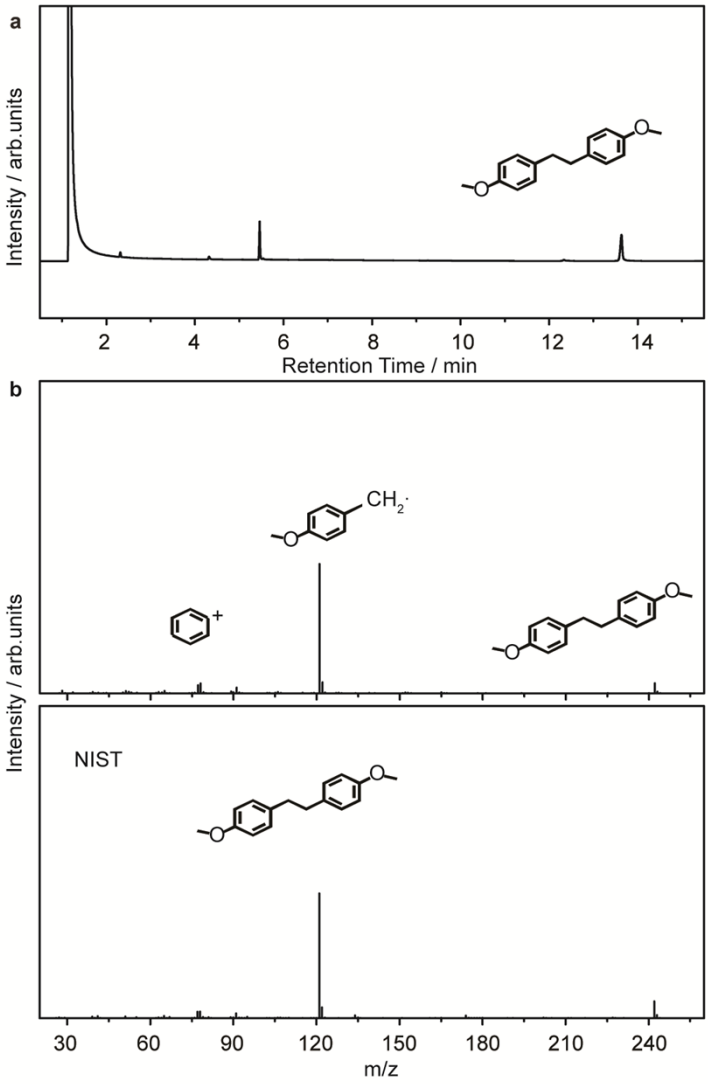

Figure S12. 4-methoxybenzyl bromide as substrate. **a** GC data. **b** MS data.

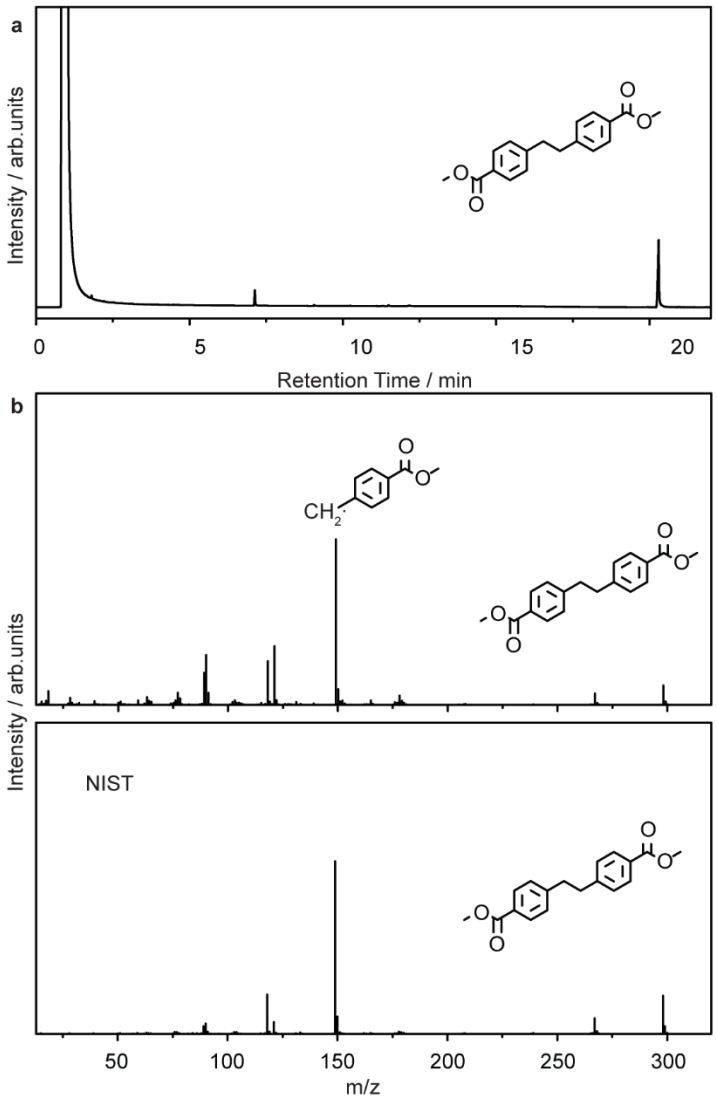

Figure S13. methyl 4-(bromomethyl)benzoate as substrate. **a** GC data. **b** MS data

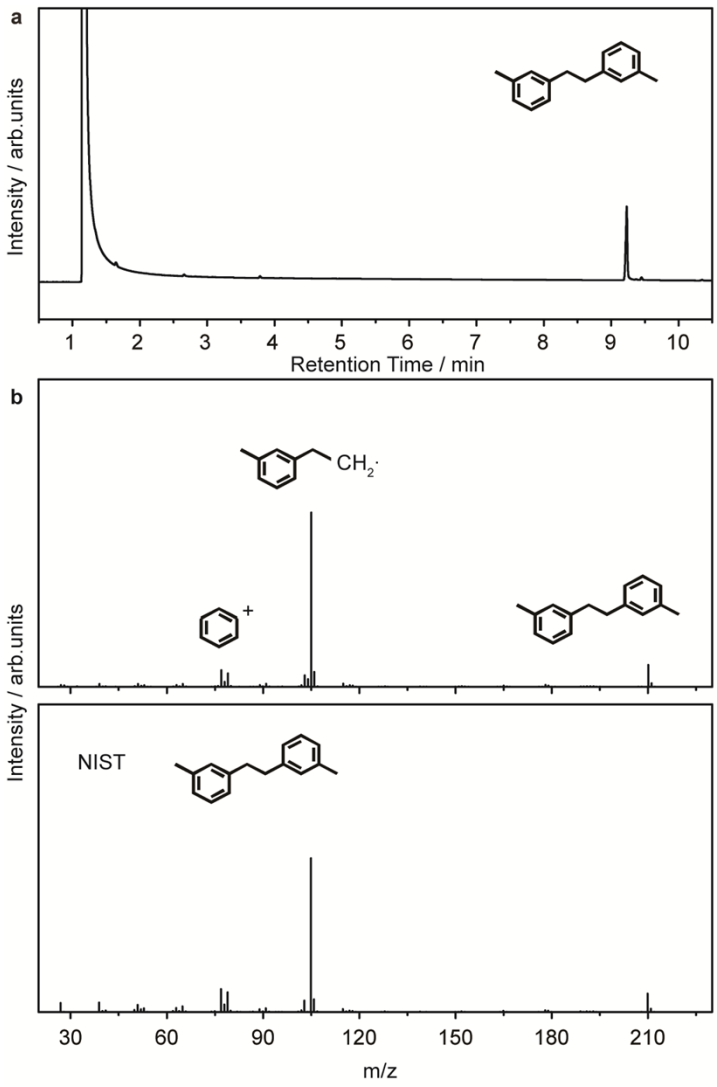

Figure S14. 3-methylbenzene bromide as substrate. **a** GC data. **b** MS data.

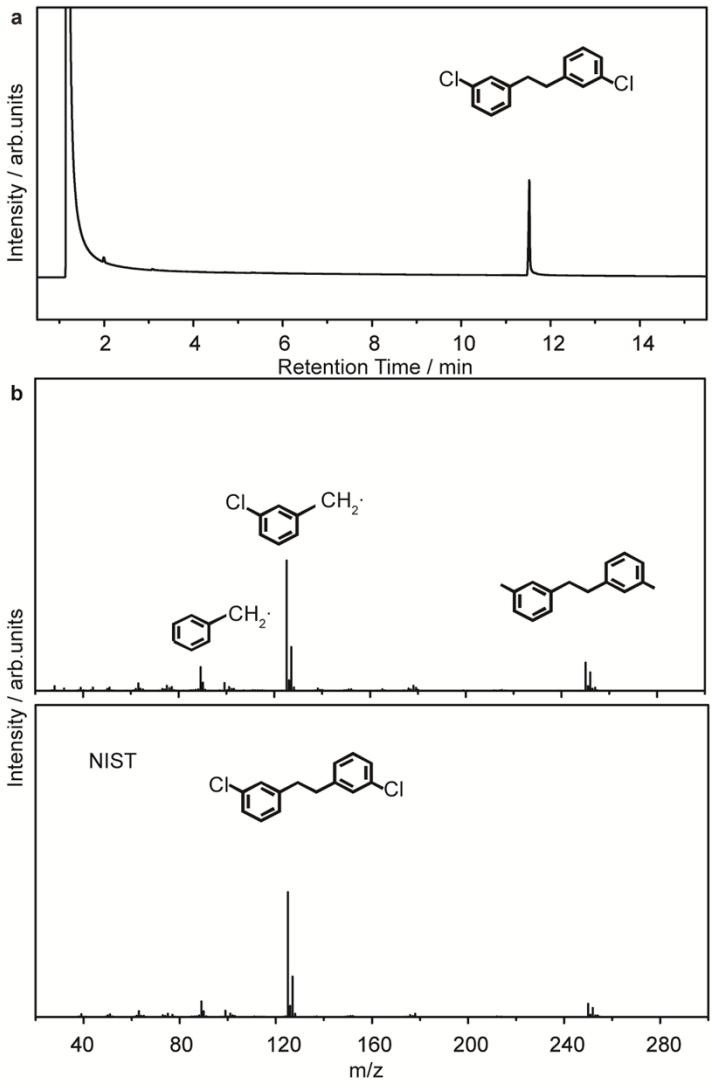

Figure S15. 3-chlorobenzyl bromide as substrate. **a** GC data. **b** MS data.

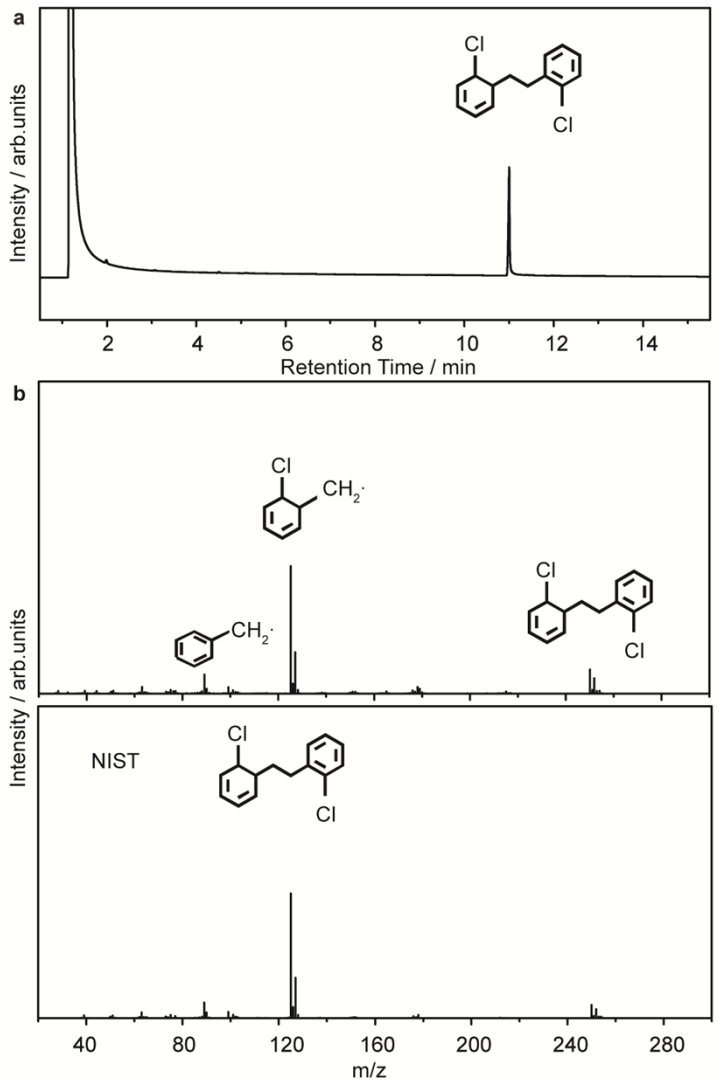

Figure S16. 2-chlorobenzyl bromide as substrate. **a** GC data. **b** MS data.

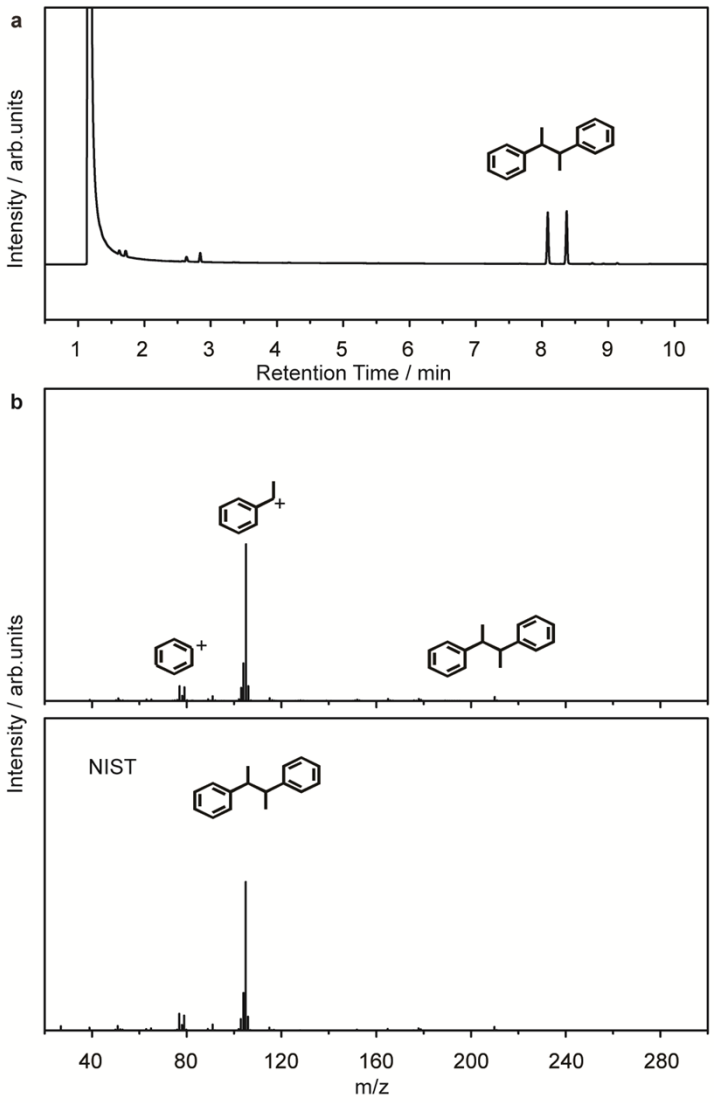

Figure S17. 1-phenethyl bromide as substrate. **a** GC data. **b** MS data.

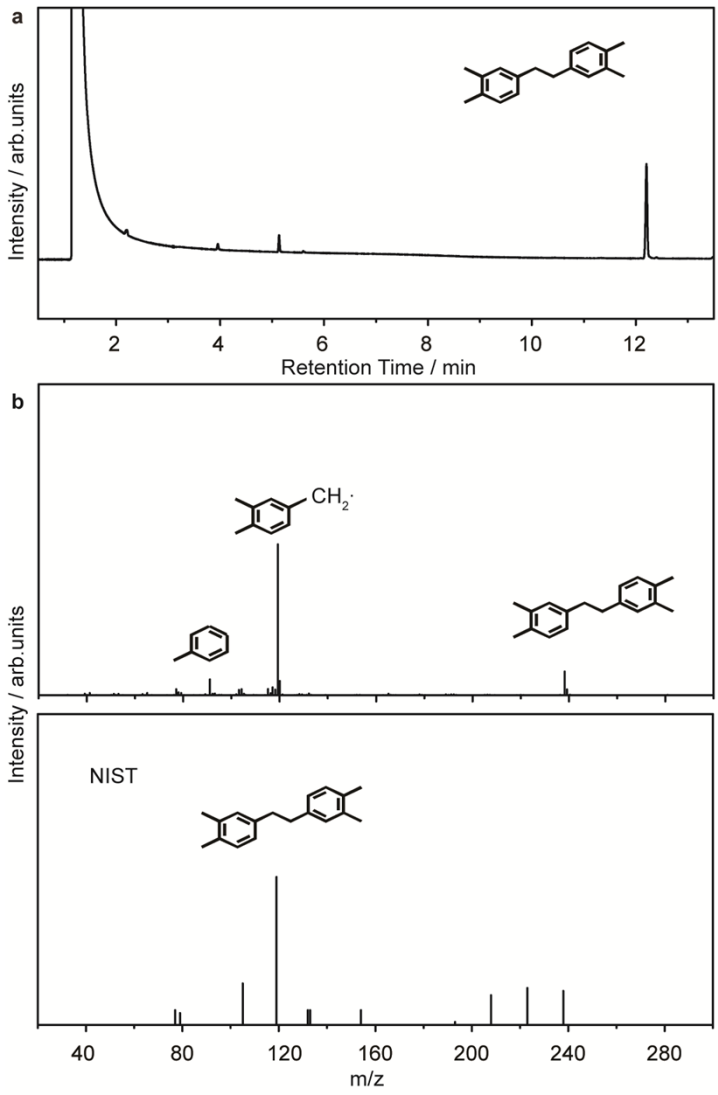

Figure S18. 3,4-dimethylbenzyl bromide as substrate. **a** GC data. **b** MS data.

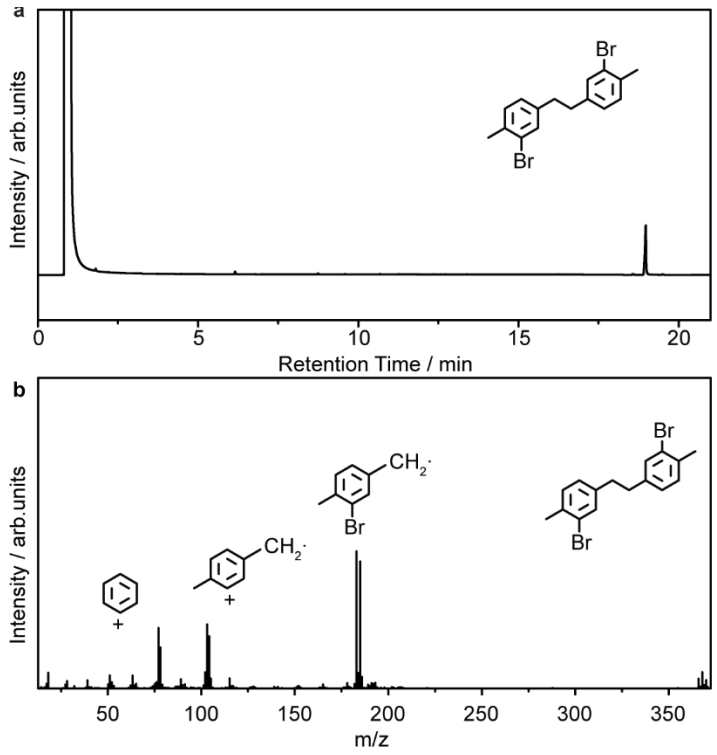

Figure S19. 2-bromo-4-(bromomethyl)-1-methylbenzene as substrate. **a** GC data. **b** MS data.

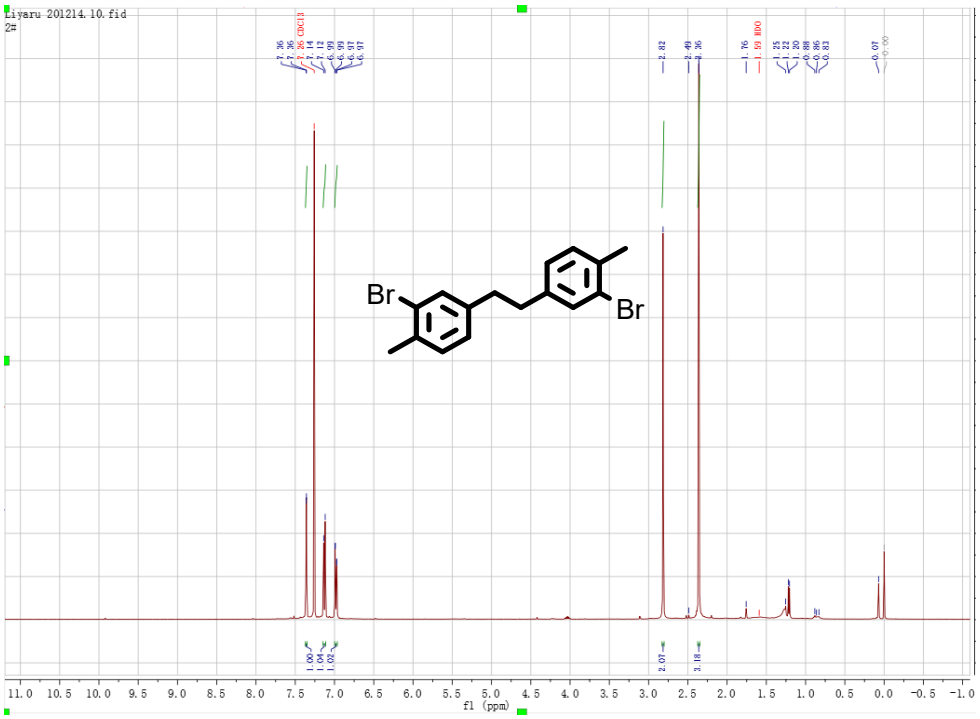

Figure S20. H spectrum (2-bromo-4-(bromomethyl)-1-methylbenzene as substrate). Reaction conditions: 8 mM of reactant, 100 mg catalyst, 15 mL isopropanol solution under vacuum, 420 nm LED lamp irradiated for 3 h, 29.5 $mW \cdot cm^{-2}$. Organic solutions were concentrated under reduced pressure on an evaporator using water bath for volatile compounds. ^1H NMR (400 MHz, $CDCl_3$) δ 7.36 (s, 2H), 7.14-7.12 (s, 2H), 6.99-6.97 (s, 2H), 2.82 (s, 4H), 2.36 (s, 6H). (Note: $CDCl_3$ referenced at 7.26 and 77.04 ppm respectively). Data for ^1H NMR are reported as follows: chemical shift (δ ppm), multiplicity (s = singlet, d = doublet, t = triplet, q = quartet, m = multiplet), integration, and coupling constant (Hz)).

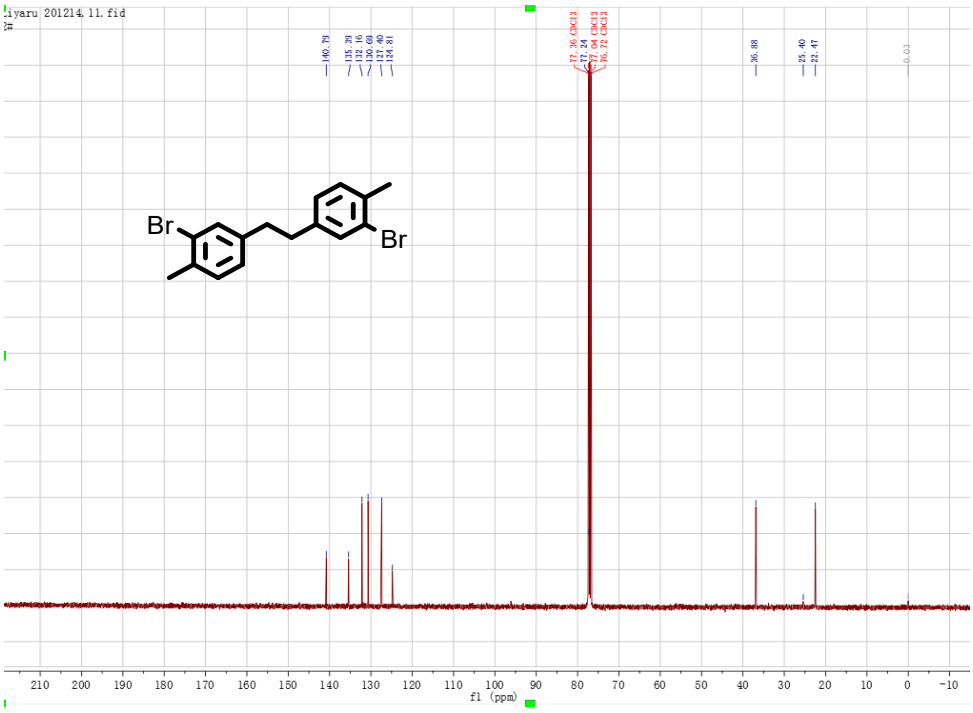

Figure S21. C spectrum (2-bromo-4-(bromomethyl)-1-methylbenzene as substrate). ^{13}C NMR (100 MHz, $CDCl_3$) δ 140.79, 135.39, 132.16, 130.69, 127.40, 124.81, 36.88, 22.47.

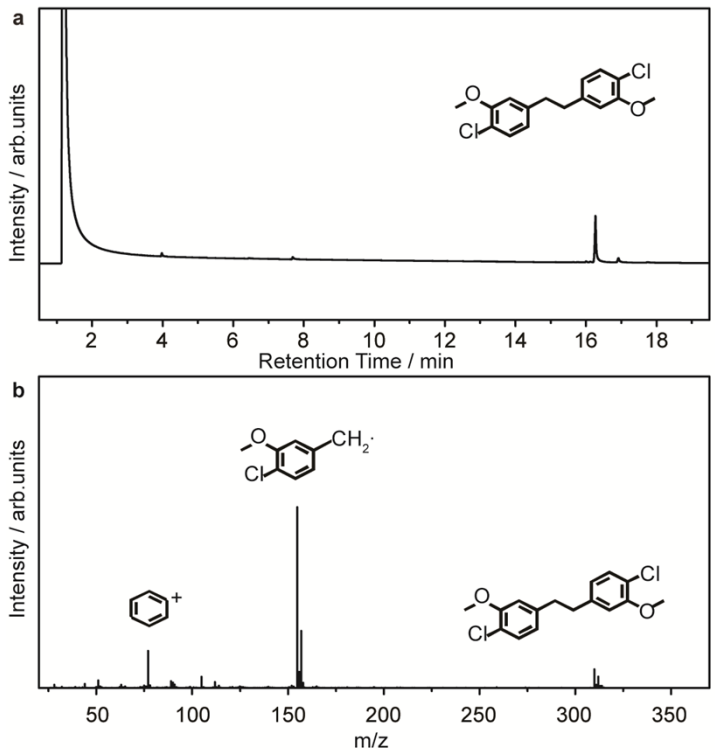

Figure S22. 4-bromomethyl-2-chloro-1-methoxy-benzene as substrate. **a** GC data. **b** MS data.

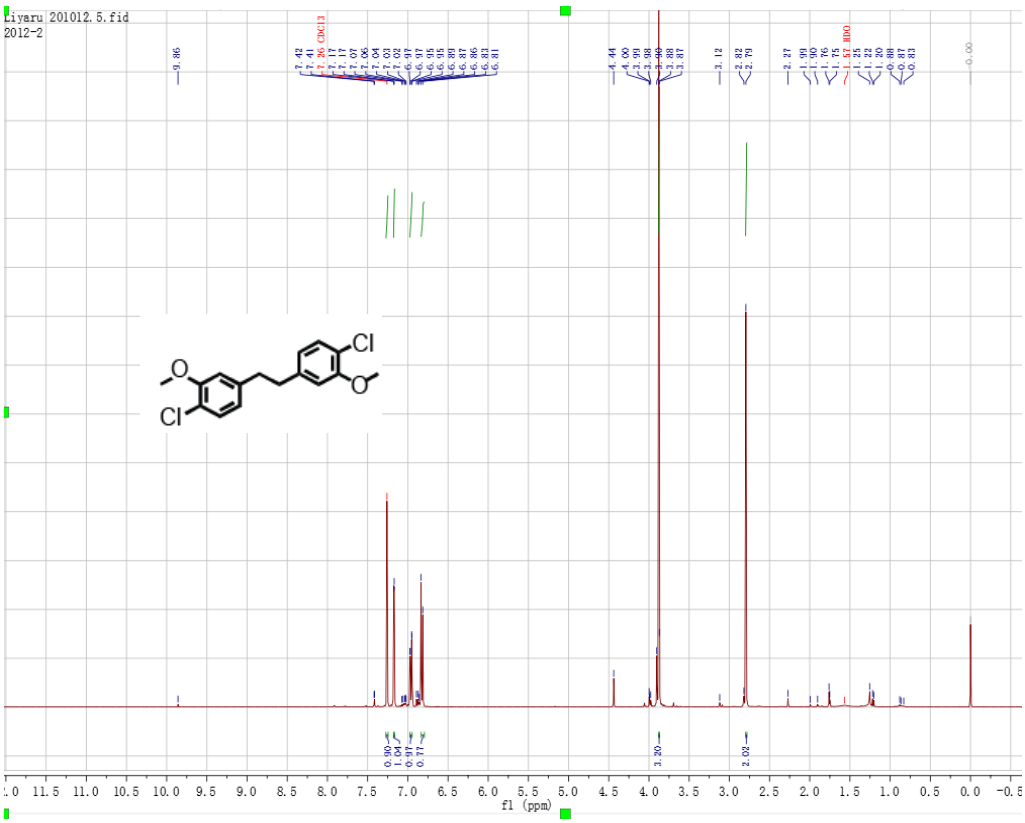

Figure S23. H spectrum (4-bromomethyl-2-chloro-1-methoxy-benzene as substrate). Reaction conditions: 8 mM of reactant, 100 mg catalyst, 15 mL isopropanol solution under vacuum, 420 nm LED lamp irradiated for 2 h, 29.5 mW·cm^{-2}. Organic solutions were concentrated under reduced pressure on an evaporator using water bath for volatile compounds. ^{1}H NMR (400 MHz, $CDCl_3$) δ7.17 (s, 1H), 6.97-6.95 (s, 1H), 6.83-6.81 (s, 1H), 3.88 (s, 3H), 2.79 (s, 2H). (Note: $CDCl_3$ referenced at 7.26 and 77.04 ppm respectively). Data for ^{1}H NMR are reported as follows: chemical shift (δ ppm), multiplicity (s = singlet, d = doublet, t = triplet, q = quartet, m = multiplet), integration, and coupling constant (Hz))

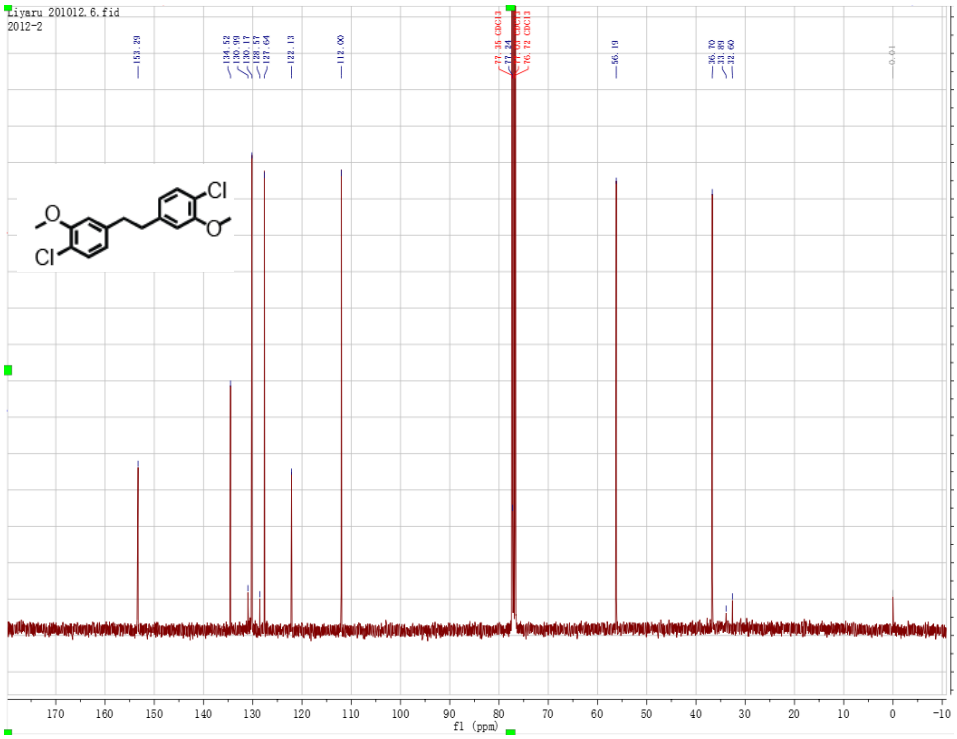

Figure S24. C spectrum (4-bromomethyl-2-chloro-1-methoxy-benzene as substrate). ^{13}C NMR (100 MHz, $CDCl_3$) δ153.29, 134.52, 130.17, 127.64, 122.13, 112.00, 56.19, 36.70.

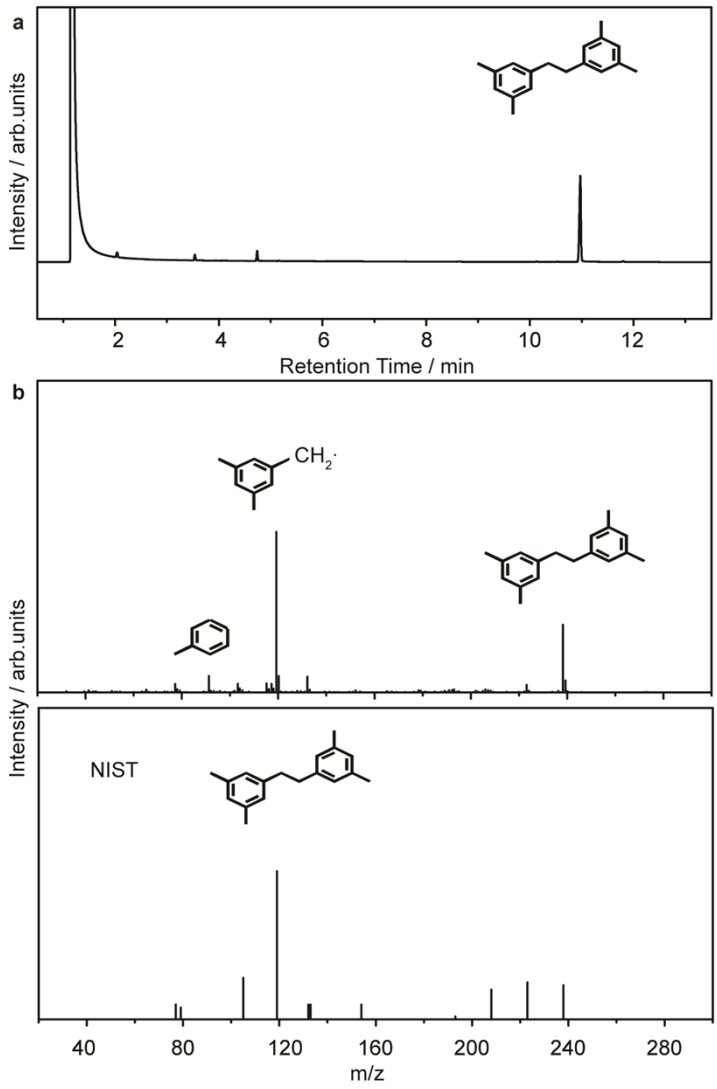

Figure S25. 3,5-dimethylbenzyl bromide as substrate. **a** GC data. **b** MS data.

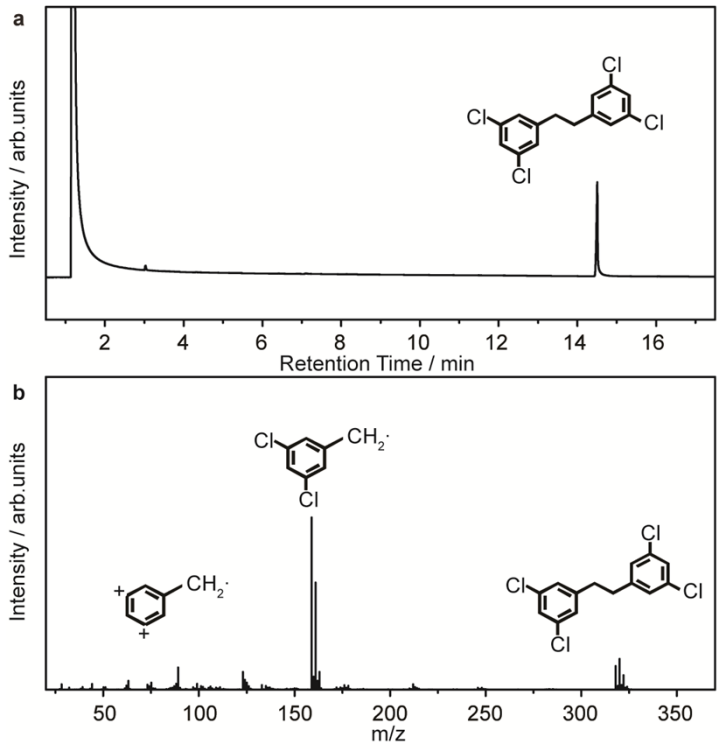

Figure S26. 1-bromomethyl-3,5-dichlorobenzene as substrate. **a** GC data. **b** MS data.

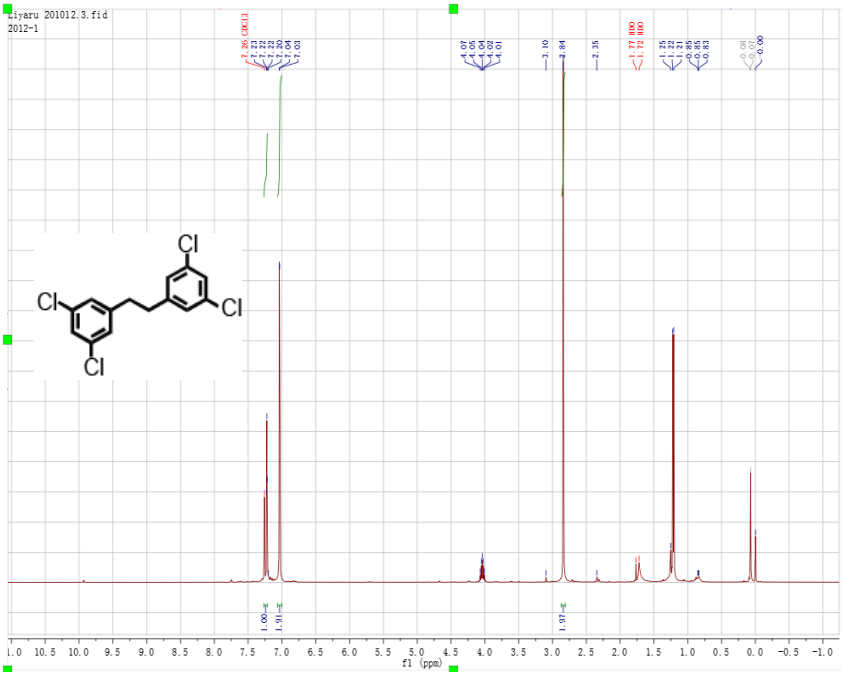

Figure S27. H spectrum (1-bromomethyl-3,5-dichlorobenzene as substrate). Reaction conditions: 8 mM of reactant, 100 mg catalyst, 15 mL isopropanol solution under vacuum, 420 nm LED lamp irradiated for 2 h, 29.5 mW·cm^{-2}. Organic solutions were concentrated under reduced pressure on an evaporator using water bath for volatile compounds. ^{1}H NMR (400 MHz, $CDCl_3$) δ 7.23-7.22 (s, 1H), 7.04-7.03 (s, 2H), 2.84 (s, 2H). (Note: $CDCl_3$ referenced at 7.26 and 77.04 ppm respectively). Data for 1H NMR are reported as follows: chemical shift (δ ppm), multiplicity (s = singlet, d = doublet, t = triplet, q = quartet, m = multiplet), integration, and coupling constant (Hz)).

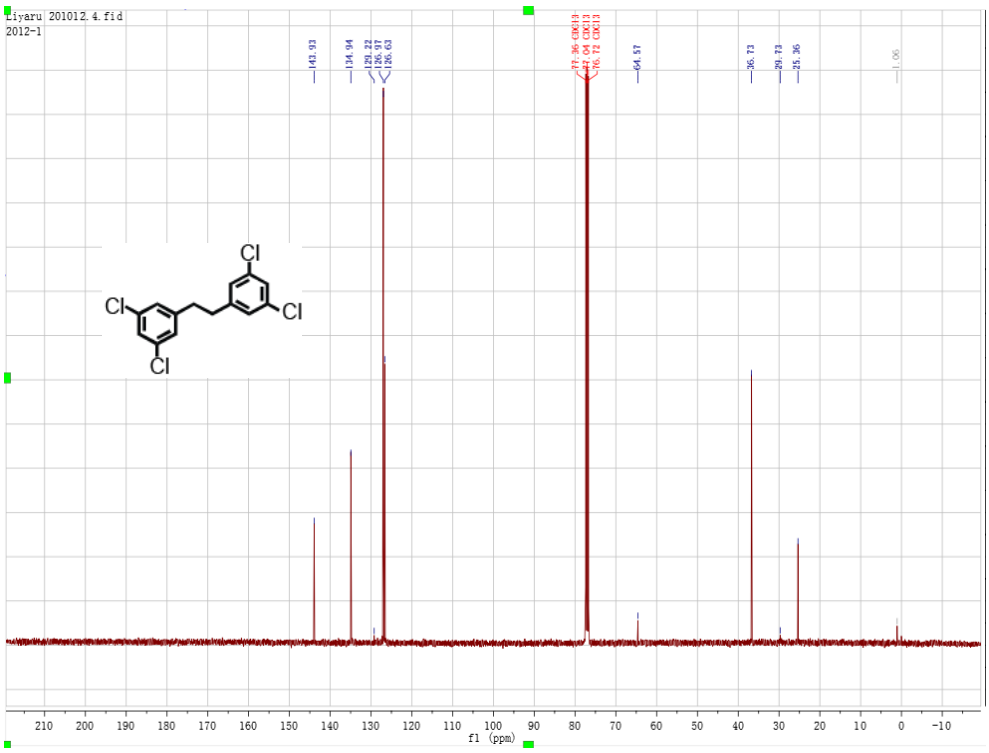

Figure S28. C spectrum (1-bromomethyl-3,5-dichlorobenzene as substrate). ^{13}C NMR (100 MHz, $CDCl_3$) δ 143.93, 134.94, 126.97, 126.63, 36.73.

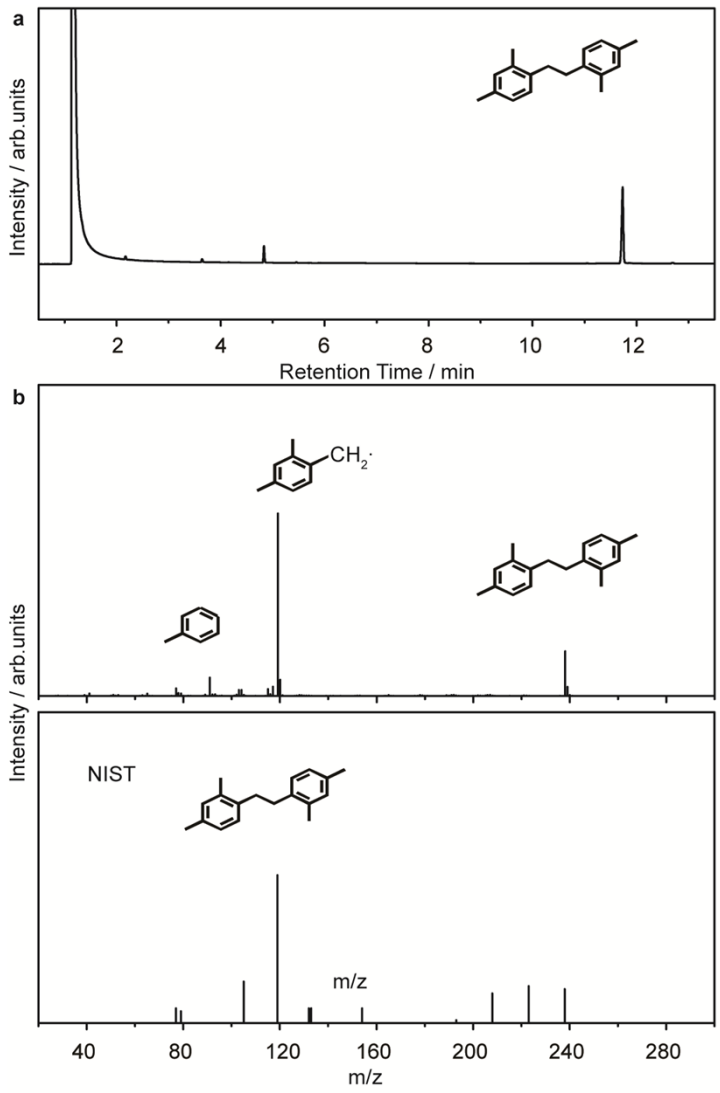

Figure S29. 2,4-dimethylbenzyl bromide as substrate. **a** GC data. **b** MS data.

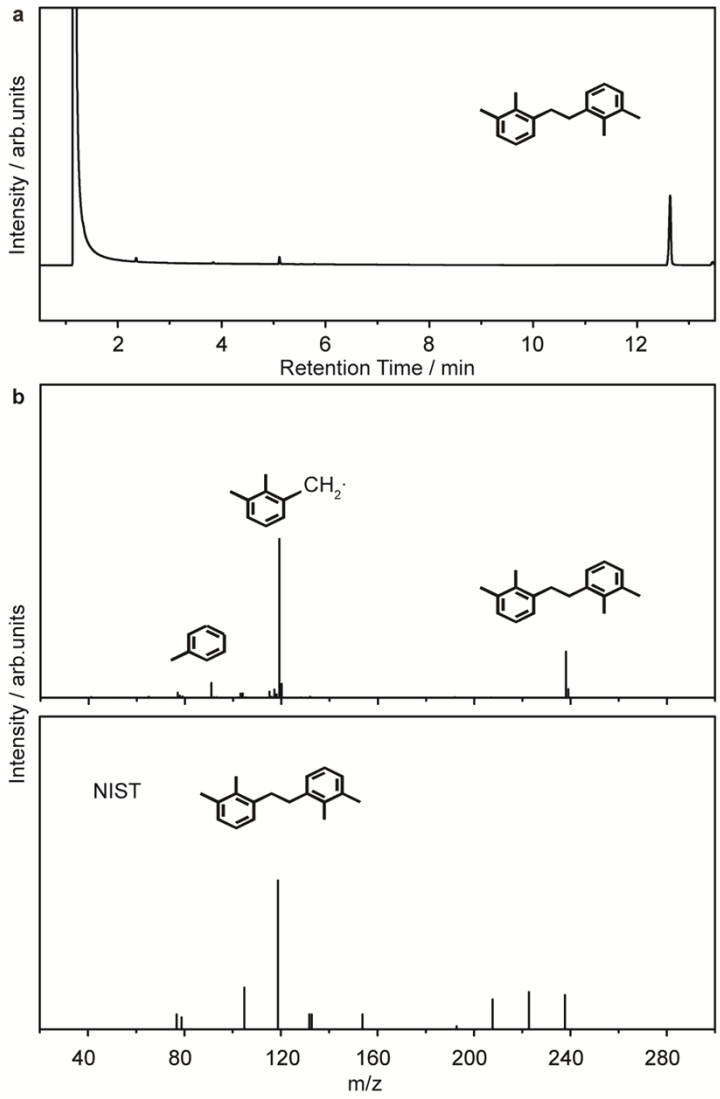

Figure S30. 2,3-dimethylbenzyl bromide as substrate. **a** GC data. **b** MS data.

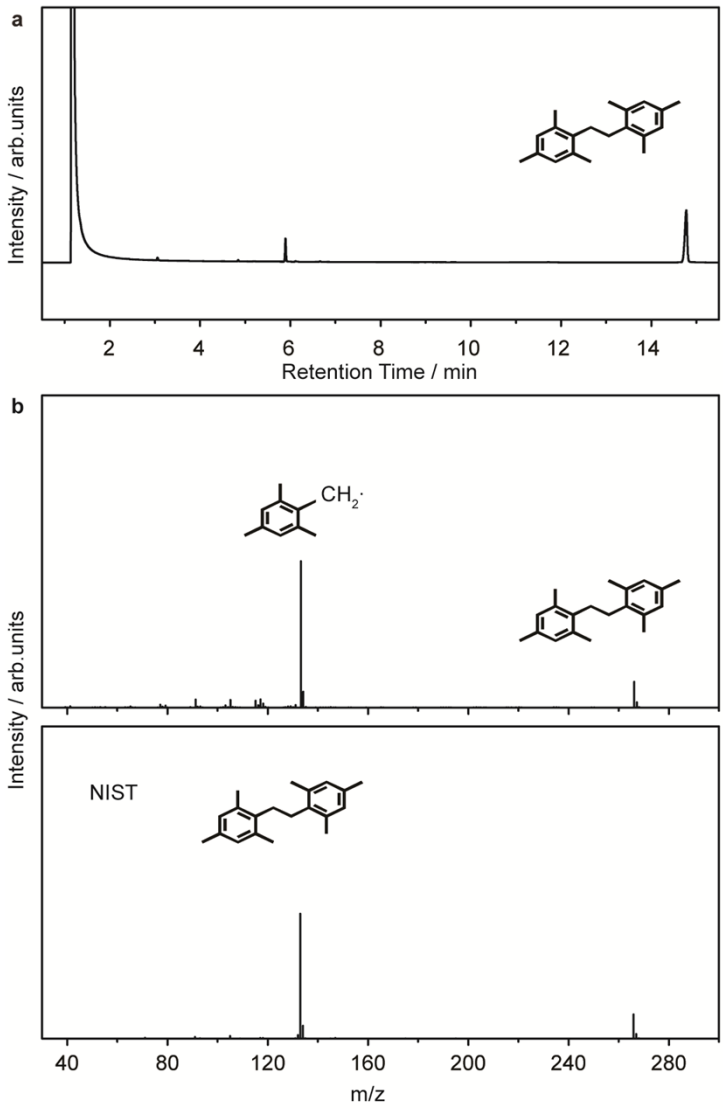

Figure S31. 2,4,6-trimethylbenzyl bromide as substrate. **a** GC data. **b** and **c** MS data.

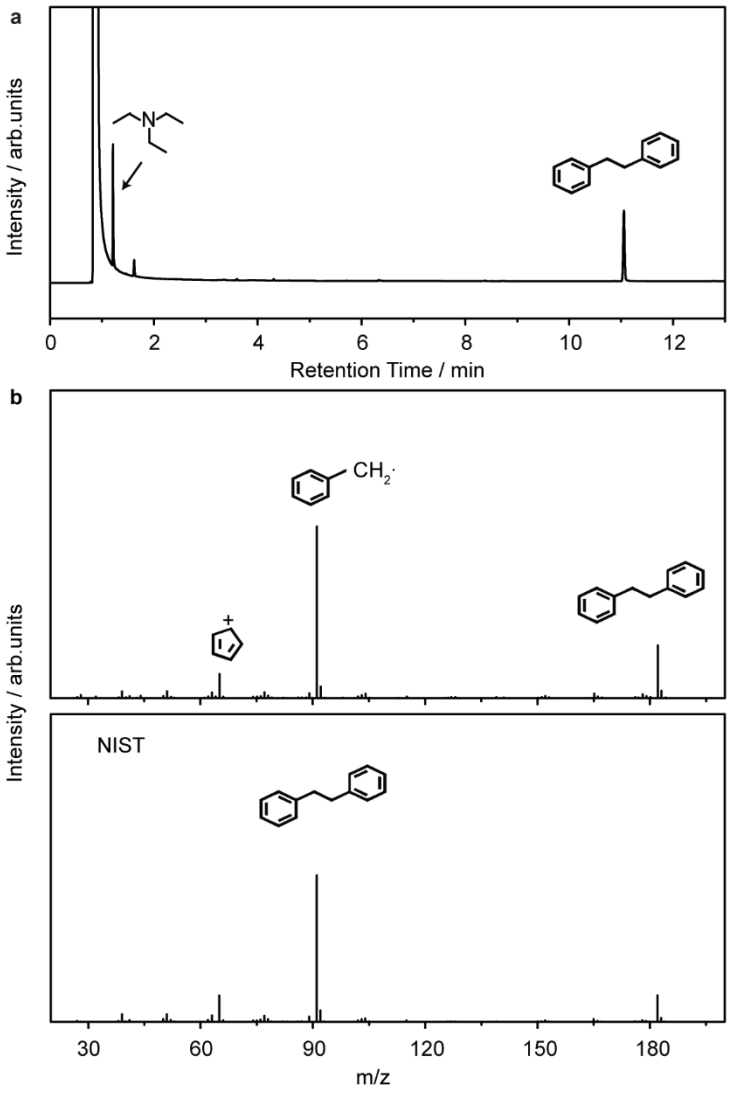

Figure S32. benzyl chloride **a** GC data. **b** MS data.

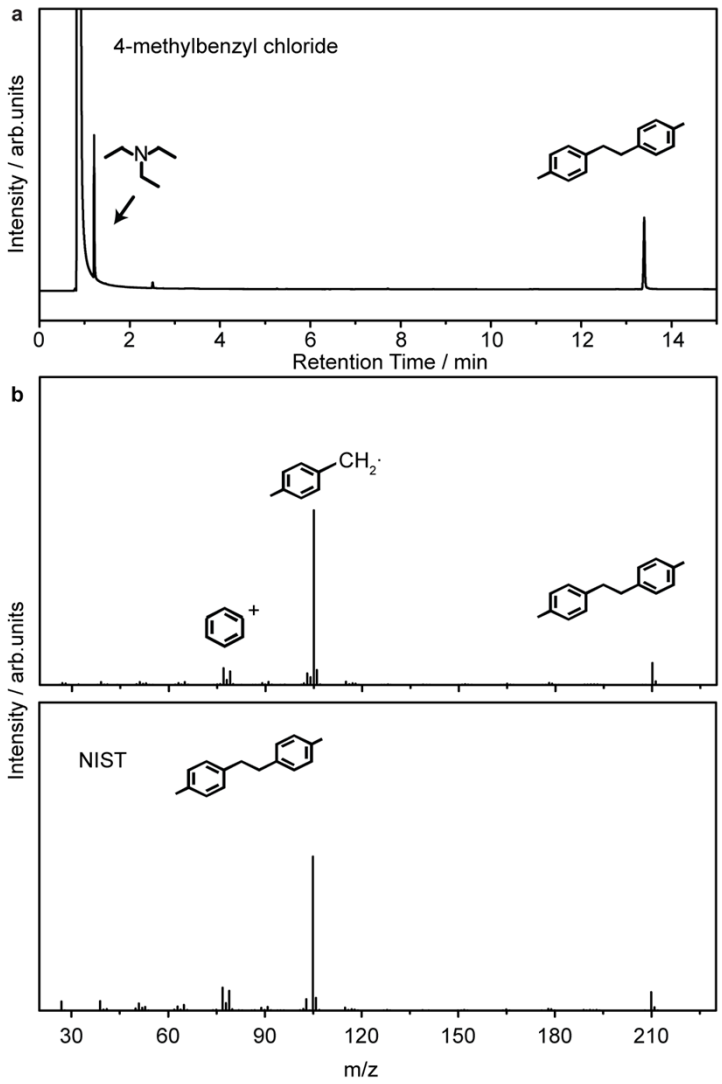

Figure S33. 4-methylbenzyl chloride **a** GC data. **b** MS data.

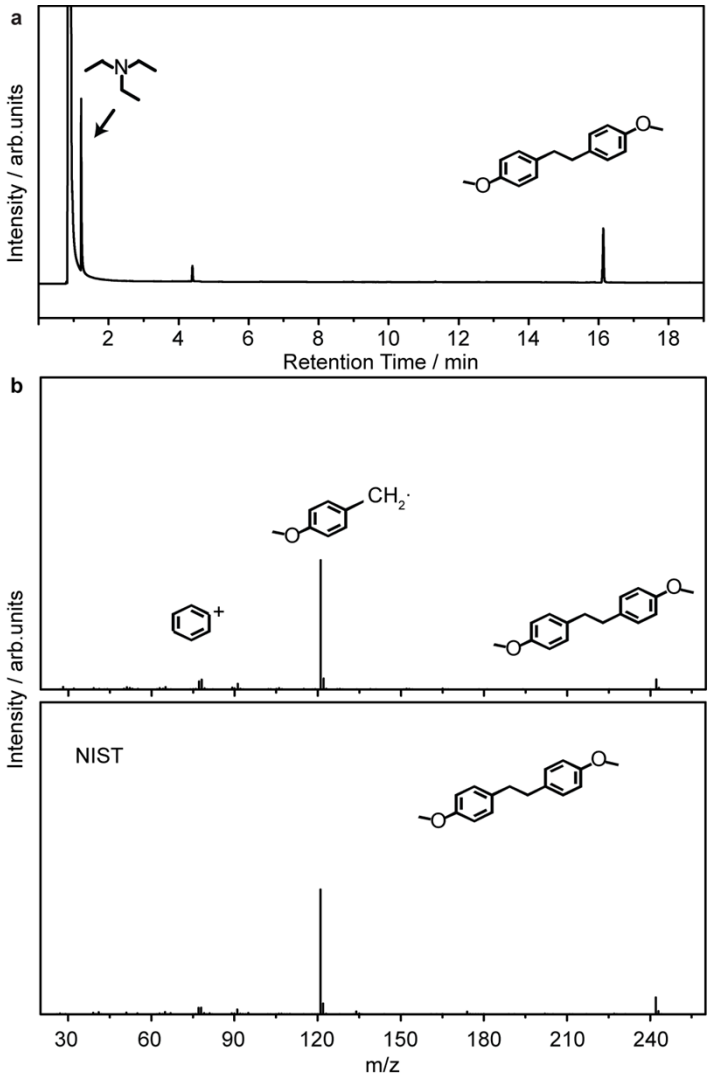

Figure S34. 4-methoxylbenzyl chloride as substrate. **a** GC data. **b** MS data.

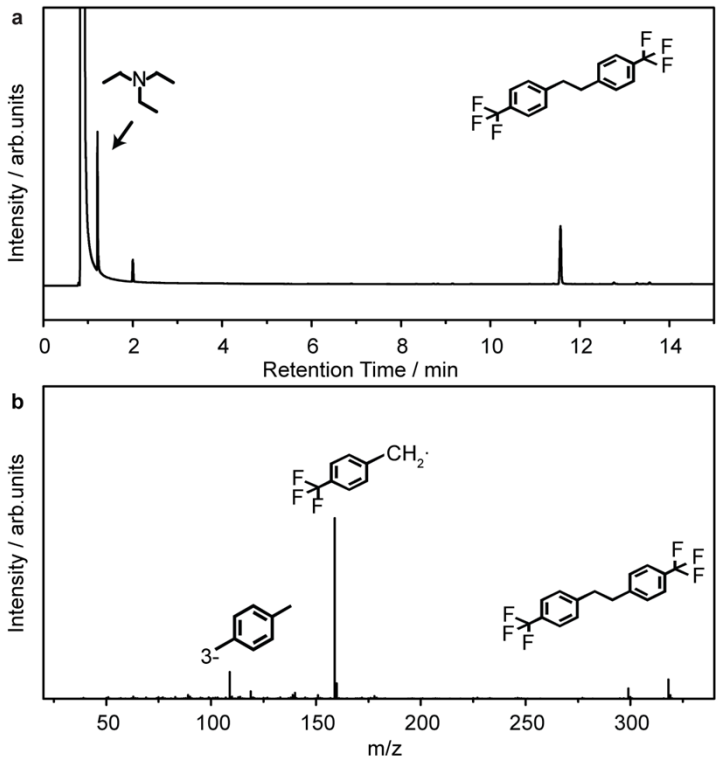

Figure S35. 4-trifluoromethylbenzyl chloride as substrate. **a** GC data. **b** MS data.

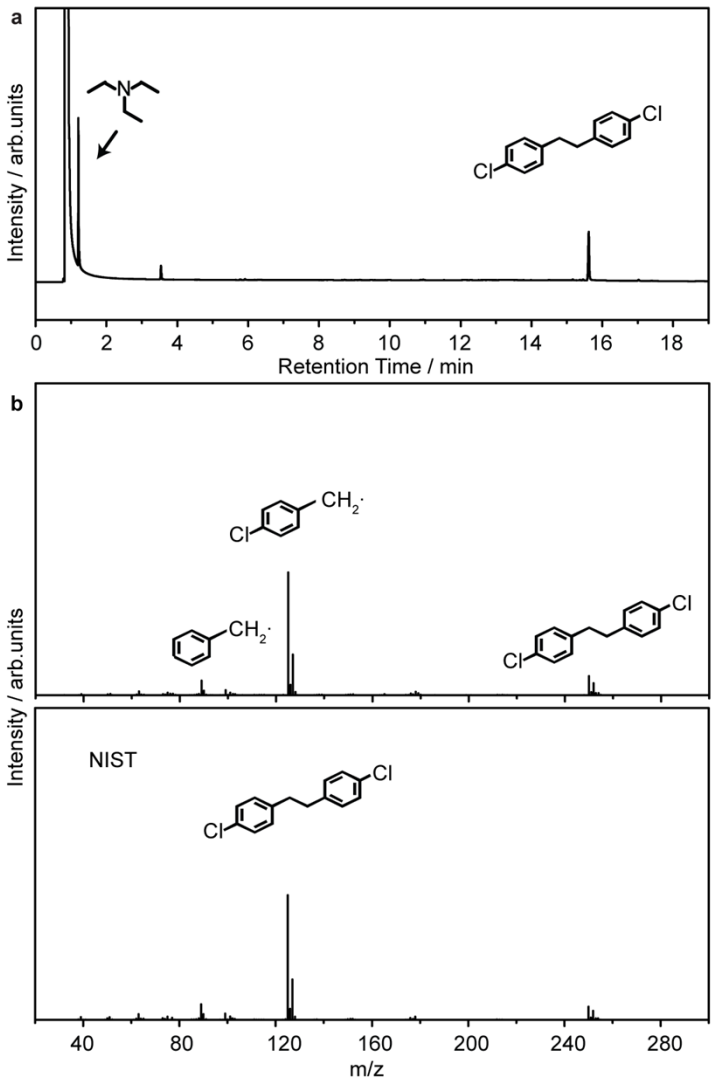

Figure S36. 4-chlorobenzyl chloride as substrate. **a** GC data. **b** MS data.

Supporting Tables

Table S1. ICP-AES analysis of metal loadings on gCN.

Catalysts	Metal / wt%	Metal / ppm
1.0 wt% Fe/gCN	1.36	13590
0.5 wt% Ru/gCN	0.54	5356
1.0 wt% Co/gCN	1.00	10000
1.0 wt% Ni/gCN	1.05	10500
1.4 wt% Rh/gCN	1.38	13810
0.9 wt% Pd/gCN	0.88	8763
0.6 wt% Pt/gCN	0.58	5762
0.3 wt% Ag/gCN	0.31	3112
0.9 wt% Au/gCN	0.89	8873
0.2 wt% Cu/gCN	0.20	1599

Table S2. Blank tests for photocatalytic homocoupling of benzyl bromide.

Entry	catalyst	Con. / %	Sel. / % (bibenzyl)
1[a]	N/A	0	0
2[a]	gCN	0	0
3[a]	$NiCl_2$	0	0
4[a]	Ni/gCN	99	85
5[b]	Ni/gCN	91	79
6[c]	Ni/gCN	0	0

General reaction conditions: 8 mM substrates and 20 mg catalyst in 3 mL isopropanol solution at RT. [a] under irradiation (420 nm, 29.5 $mW \cdot cm^{-2}$) in deaerated conditions (N_2). [b] under irradiation (29.5 $mW \cdot cm^{-2}$) in aerated conditions. [c] Dark. All reaction time are 2 h.

Table S3. Survey of solvent for photocatalytic benzyl bromide conversion

Entry	Catalyst	Solvent	Con. / %	Sel. / % (bibenzyl)
1	Ni/gCN	isopropanol	99	85
2	Ni/gCN	ethanol	88	89
3	Ni/gCN	n-hexane	5	30
4	Pd/gCN	n-hexane	14	0
5	Ni/gCN	CH_2Cl_2	10	69
6	Ni/gCN	acetonitrile	3	0
7	Pd/gCN	acetonitrile	10	0
8	Ni/gCN	cyclohexane	6	36

General reaction conditions: 8 mM substrates, 29.5 $mW \cdot cm^{-2}$ light intensity, and 20 mg catalyst in 3 mL solvent under deaerated condition at RT for 2 h.

Reference:

1 C. Garlisi, G. Scandura, J. Szlachetko, S. Ahmadi, J. Sa, G. Palmisano, *Appl. Catal., A,* 2016, **526**, 191-199.

2 Y. Lei, X. Lei, P. Westerhoff, X. Tong, J. Ren, Y. Zhou, S. Cheng, G. Ouyang, X. Yang, *Environ. Sci. Technol.,* 2022, **56**, 5189-5199.

3 R. Su, R. Tiruvalam, A.J. Logsdail, Q. He, C.A. Downing, M.T. Jensen, N. Dimitratos, L. Kesavan, P.P. Wells, R. Bechstein, H.H. Jensen, S. Wendt, C.R.A. Catlow, C.J. Kiely, G.J. Hutchings, F. Besenbacher, *ACS Nano*, 2014, **8**, 3490-3497.